AIDIC CONFERENCE SERIES

A publication of AIDIC
The Italian Association of Chemical Engineering
www.aidic.it/acos

VOL. 11, 2013
Chief Editor: Sauro Pierucci

ISBN 978-88-95608-55-6; **ISSN** 2036-5969

DOI: 10.3303/ACOS1311036

Effect of Different Viscosity on Optimal Shape of Static Mixers for Food Industry

Fabrizio Sarghini*, Annalisa Romano , Paolo Masi

CAISIAL, Department of Agriculture, University of Naples Federico II, Italy.
Via Università 100, 80055 Portici (NA), Italy.
fabrizio.sarghini@unina.it

Mixing is a common process in food industry, and in particular it is interesting to develop optimal mixers in order maximize fluid mixing and minimize energy consumption by reducing the viscous dissipation effects. Although many studies and results had been presented in literature for both batch and static mixers (Rauline et al. 2000 and Mutsakis et al. 1986 for a review) the lack of a developed theory of instability for non-Newtonian fluids, quite common in the food industry, leaves the problem open.
In this work, the Optimal Shape Design (OSD) technique was applied to design static mixers for a Newtonian (i.e., water) and pseudoplastic (i.e., peach puree) liquid. Results show for the Non-Newtonian case, a classical coaxial static mixer, the application of OSD allows a sensible improvement of the performances, while in the Newtonian case (High Efficiency Vortex mixer), due to the different design approach, the overall effects are negligible.

1. Introduction

Static mixers can be considered standard equipment in the chemical and food industry, and they are employed inline in a once-passing process or in a recycle loop where they can replace or supplement a conventional agitator.
Their use is an attractive alternative to conventional agitation since similar and sometimes better performance can be achieved at lower cost, as they typically have lower energy consumptions and reduced maintenance requirements because they have no moving parts. Moreover they offer a scalable rate of dilution in fed batch systems and can provide homogenization of feed streams with a minimum residence time (Thakur et al, 2003). Literature is overwhelming: there are more than 8000 paper and about hundred commercial types.
Despite the wide use of this device, the basic design approach is still partially linked to case by case experiments and a general procedure to optimize their performance is still missing.
The prototypical design of a static mixer can be described by a series of identical motionless inserts (elements) installed in pipes, columns, or reactors. The purpose of such elements is to redistribute the fluid in the radial and tangential directions with respect to the main flow, while the effectiveness of this redistribution is a function of the specific design and number of elements.
A typical example is the Kenics static mixer, representing a widely used device in the food and chemical industries including a composite variety of mixing applications such as liquid–liquid dispersion or gas–liquid dispersion ((Hobbs and Muzzio, 1998a,b; Hobbs et al., 1998; Byrde and Sawley, 1999; Rauline et al., 2000; Fourcadeet al., 2001; Szalai and Muzzio, 2003; van Wageningen etal., 2004).
The particular configuration of the mixing elements allows periodic splitting and remixing at the junctions and stretching and folding within the elements, but despite the effectiveness of the Kenics static mixers, their use is often restricted due to the large pressure drop caused by the helical elements, where the mixing strength of the mixers is achieved at the expense of high pressure drop.
Moreover, another parameter affecting the final pressure drop for unit of length is given by the effect of viscosity for Non-Newtonian fluids, being viscosity dependent on the local shear rate.

Please cite this article as: Sarghini F., Romano A., Masi P., 2013, Effect of different viscosity on optimal shape of static mixers for food industry, AIDIC Conference Series, 11, 351-360 DOI: 10.3303/ACOS1311036

A compromise configuration could be obtained trying to maximize mixing with minimum pressure drop with an appropriate shape of the mixing elements.
To this purpose, computational fluid dynamics can be considered an important tool to analyze their performance and to optimize their configurations. More specifically, the Optimal Shape Design (OSD) (Mohammadi and Pironneau, 2001) is a technique capable of designing automatically an optimal functional shape by solving the Navier-Stokes for a non-Newtonian fluid with reference to a geometrical shape that is a part of the degrees of freedom of the problem under study.
Tartar (1994) analyzed stability and existence of the solution, showing that the problem is ill posed in many practically important situation, and then leading thereby to the introduction of relaxed problems known as topological optimization.
Nonetheless, OSD still presents numerically difficulties, as it is computer intensive and because in practice one has to make compromises between shapes that are good with respect to more than one criteria. One approach is via Pareto optimality, using a mathematical theorem stating that in simple situations Pareto optimal points are minimizers of some convex combination of all the criteria, although sometimes linear combinations lead to stiff problems with many sub-optima, requiring global optimization tools such as genetic algorithms (Mohammadi and Pirennau,2004).
The main aim of this work was to compare the optimal configurations of the static mixers used to deal with typical Newtonian and non-Newtonian food liquids as resulting from the OSD approach.
.

2. Numerical methods

Mass- and momentum-conservation laws provide the governing equations to solve isothermal incompressible-flow problems:

$$\nabla \cdot (\boldsymbol{u}) = 0 \tag{1}$$

and momentum conservation

$$\frac{\partial(\rho \mathbf{u})}{\partial t} + \nabla \cdot (\boldsymbol{\rho u\, u}) = -\nabla p + \nabla \cdot \boldsymbol{\tau} \tag{2}$$

where ρ is the density of the fluid, u the velocity vector, p the pressure, and τ the stress tensor.
These are to coupled to a constitutive equation to relate the stress and deformation rate for the fluid of interest. In this work, the stress tensor for the non-Newtonian fluid tested was described by the well known Ostwald–de Waele relationship:

$$\tau = k\dot{\gamma}^n \tag{3}$$

with

$$\dot{\gamma} = \sqrt{\frac{1}{2}(\overline{\boldsymbol{D}}:\overline{\boldsymbol{D}})} \tag{4}$$

and

$$\mathbf{D} = \frac{1}{2}(\nabla \mathbf{u} + [\nabla \mathbf{u}]^T) \tag{5}$$

Given the initial fields of velocity **u**, pressure *p*, and stress ***τ***, the explicit calculations of the pressure gradient and the stress divergence are carried out, and then the momentum equation is solved implicitly for each component of the velocity vector, thus computing a new estimate of the velocity field $\mathbf{u}^*$. In sequence, the new pressure field p^* is estimated leading to a new velocity field $\mathbf{u}^{**}$ which satisfies the continuity equation. Several algorithms like SIMPLE (Patankar and Spalding, 1972) or PISO (Issa,1986) can be used to obtain p^* and $\mathbf{u}^{**}$, even if PISO is regarded as the best option for transient flows (Burton, 1998).
The corrected velocity field $\mathbf{u}^{**}$ give rise to a new estimate $\boldsymbol{\tau}^*$ for the stress tensor field is calculated by solving the specified constitutive equation.

Such steps may be recursively repeated within each time step in order to generate more accurate solutions in transient flows. To this numerical framework, a moving mesh approach is introduced to compute the Optimal Shape Design (OSD)
With respect to classical numerical simulations in fixed geometrical configurations, such algorithm introduces a certain number of geometrical degrees of freedom (d.o.f.) as a part of the unknowns, which means that the geometry is not completely defined in a static configuration, but part of it is allowed to move dynamically to minimize an objective function which defines a target of a constrained minimum problem.
The second step is the choice of an appropriate non-linear multivariate minimization algorithm. In general, genetic algorithms can be used in the case of multiple local minimum configuration (Obayashi, 1997), while in presence of single global minimum a gradient-based approach (such as the steepest-descent one) is preferred (Sokolowski and Zolezio,1991).
In this paper a sensitivity analysis approach, based on numerical computation of the gradient matrix was chosen; more in details, we used a variable metrics Quasi-Newton approach, based on the Broyden-Fletcher-Goldfarb-Shanno (BFGS) algorithm (Keller, 1999).
The BFGS method approximates Newton's method, seeking a stationary point of a preferably twice continuously differentiable function, and it has proven to have good performance even for non-smooth optimizations
The advantage of Quasi-Newton method is that the Hessian matrix of second derivatives doesn't need to be evaluated directly, and the Hessian matrix is approximated using rank-one updates specified by gradient evaluations.
By defining:

$\bar{\mathbf{x}}$ as the vector of fixed geometrical nodes; (6)

$\mathbf{x}_n^k$ as the vector of the moving geometrical d.o.f.; (7)

$\mathbf{G}(\bar{\mathbf{x}}, \mathbf{x}_n^k)$ as the integral of the target objective function $\mathbf{I}(\bar{\mathbf{x}}, \mathbf{x}_n^k)$(see Eq. (18) and Eq. (19)); (8)

$\mathbf{F}(\bar{\mathbf{x}}, \mathbf{x}_n^k)$ as the system of state equations previously described; (9)

$\mathbf{x}_n^k : \{s_1(\mathbf{x}_n^k) < \mathbf{x}_n^k < s_2(\mathbf{x}_n^k)\}$ as the geometrical constrains, (10)

The OSD algorithm may be described as follows:
:

a) solve $\mathbf{F}(\bar{\mathbf{x}}, \mathbf{x}_n^k) = 0$ (11)

b) compute the Jacobian $J = \frac{\partial \mathbf{F}(\bar{\mathbf{x}}, \mathbf{x}_n^k)}{\partial \mathbf{x}_n^k}$; (12)

c) find $\beta : \left\{\int_\Omega \mathbf{I}(\bar{\mathbf{x}}, \mathbf{x}_n^{k+1}) d\boldsymbol{\Omega} < \int_\Omega \mathbf{I}(\bar{\mathbf{x}}, \mathbf{x}_n^k) d\boldsymbol{\Omega}\right\}$ by using a linesearch algorithm (Nocedal,2006); (13)

d) $\mathbf{x}_n^{k+1} = \mathbf{x}_n^k + \boldsymbol{\beta}$ (14)

e) if $\left(\int_\Omega \mathbf{I}(\bar{\mathbf{x}}, \mathbf{x}_n^{k+1}) d\boldsymbol{\Omega} - \int_\Omega \mathbf{I}(\bar{\mathbf{x}}, \mathbf{x}_n^k) d\boldsymbol{\Omega}\right) < \varepsilon$, with e being a prefixed error;
then $\mathbf{x}_n^{k+1} = \mathbf{x}_{optimal}$ otherwise reiterate from step (a) (15)

In the OSD problems, geometry is allowed to be modified according to the minimum of the object function. If we consider all computational grid points on the moving surface as unknowns, the computational weight will soon become overwhelming, and a possible solution is to consider a control grid with a limited number of moving points (the geometrical unknowns part of the OSD problem), and a smooth mapping algorithm from the computational plane to the physical plane in order to reconstruct the numerical grid after control geometry movements and smoothing.

The grid points Pz are allowed to move on circular trajectories on fixed z-planes (fig. 1a), introducing a geometrical constrain for the generic n-iteration defined as

$$\alpha_n(P_z) - \alpha_0(P_z) \in [-\alpha, +\alpha] \tag{16}$$

In this way the only varying parameter for each control point is α, but nonetheless a generalized optimal 3D surface can be obtained.
Once the new control points positions at the next iteration n+1 are known, the related positions of computational mesh points are recovered by using a surface patch via a finite-element representation of α in terms of reference coordinates (ζ, ξ).
The initial position of each computational and control node , $\mathbf{P}z\ (r_0, z_0)$ is mapped into the reference plane $P(\zeta_0, \xi_0)$, with $(\zeta, \xi)\ \varepsilon[-1,+1]$ using a second order 12 nodes serendipity type finite element (fig. 1b); as the control points are allowed to move only on a circular trajectory, their positions on the reference plane (ζ, ξ) remain unchanged, and any variation of α imposed by the minimization algorithm is mapped back from the reference plane to the physical plane for all remaining computational nodes.

The values for each sub-control node, (i.e. the intermediate nodes) on each element side in the reference plane, are obtained by using a tensor product B-Spline representation (Farin, 2001).

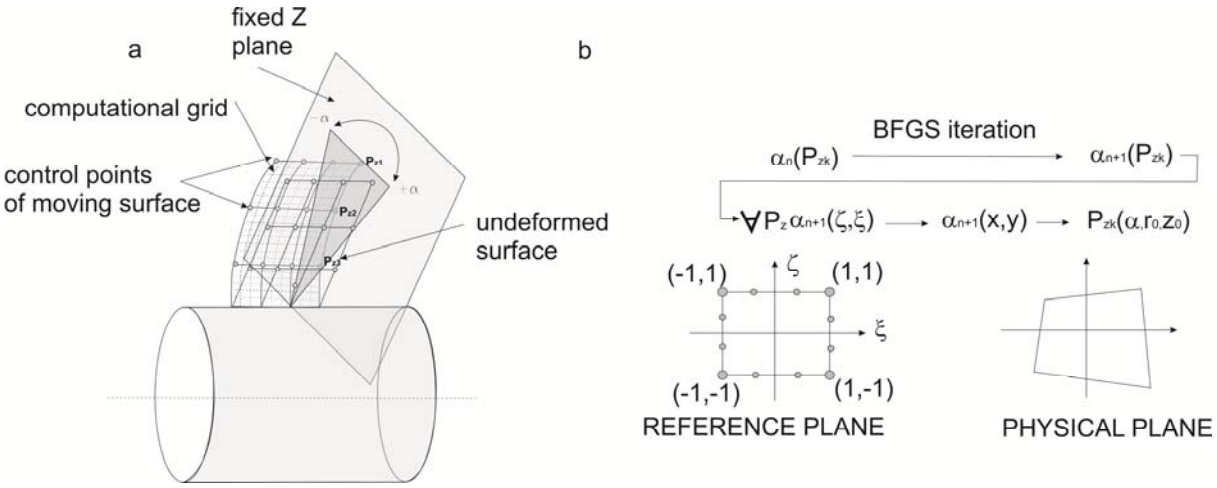

Figure 1: Control points for the static mixer (a) and mapping of α angle from reference to physical plane (b).

Mixing effects were computed by introducing at the inflow boundary a numerical non diffusive passive scalar $F(\mathbf{x})$ from several slots (Figure 2). Introducing the average scalar concentration $\bar{\Phi}$ as

$$\bar{\Phi} = \Phi_{in} \frac{\mu(\Omega_{slot})}{\mu(\Omega_{out})} \tag{17}$$

where $\Phi_{in} = 1$ is the scalar concentration at the inflow, while $\mu(\Omega_{slot})$ and $\mu(\Omega_{out})$ are the measures of the scalar inflow and outflow surfaces, we can compute a numerical convex mixing index **M**

$$\mathbf{M} = \int_{\Omega_{out}} \left(\bar{\Phi} - \Phi(\bar{\mathbf{x}}, \mathbf{x}_n^k)\right)^2 d\Omega \tag{18}$$

Moreover, we can define the integral of the quadratic object function averaged over time length $\Delta t = t_2 - t_1$

$$G_1(\bar{x}, x_n^k) = \frac{1}{\Delta t}\int_{t_1}^{t_2} \int_{\Omega_{out}} \left(\bar{\Phi} - \Phi(\bar{x}, x_n^k)\right)^2 \, d\Omega dt \tag{19}$$

At the same time, pressure drop was also checked, as the target of improving mixing should be coupled to a limited increase in terms of pressure drop.
In fact, the shear stress dissipative work was considered by computing the pressure drop between inflow and outflow boundaries, as

$$G_2(\bar{x}, x_n^k) = \frac{1}{\Delta t}\int_{t_1}^{t_2} \left[\int_{\Omega_{out}} P(\bar{x}, x_n^k)\, d\Omega - \int_{\Omega_{in}} P(\bar{x}, x_n^k)\, d\Omega \right] dt \tag{20}$$

In order to consider both effects in the OSD algorithm, a linear composite objective function was chosen between many possibilities according to the following form:

$$G(\bar{x}, x_n^k) = 0.5\frac{G_1(\bar{x}, x_n^k)}{G_1(\bar{x}, x_0^1)} + 0.5\frac{G_2(\bar{x}, x_n^k)}{G_2(\bar{x}, x_0^1)} \tag{21}$$

In the case of a constrained minimum problem, the choice of the geometrical constrains strongly influences the "optimal" geometric configuration, which must be considered a local relative optimum.
The numerical solver adopted in this work is OpenFoam (OpenFoam v2.2.0), a free, open source CFD software package. Several mesh configurations were tested, ranging from $300x10^3$ up to $1.5x10^6$ control volumes, and grid independence was tested on fixed geometry cases. A Large Eddy Simulation approach was used for turbulent cases using a scale similar model (Sarghini et al, 1999, Sarghini et al. 2003 for the implementation).

For each iteration the simulation final time t_2 was set considering the physical requirements to allow the tracer to reach the outflow in the new configuration, depending on the average velocity of the volumetric flow rate.

3. Results

Two different module geometries were investigated, they correspond to a High Efficiency Vortex static mixer (see Ghanem *et al.*, 2013 for a review) and a coaxial static mixer, whose initial configuration are shown in Figure 2a and 2b respectively.

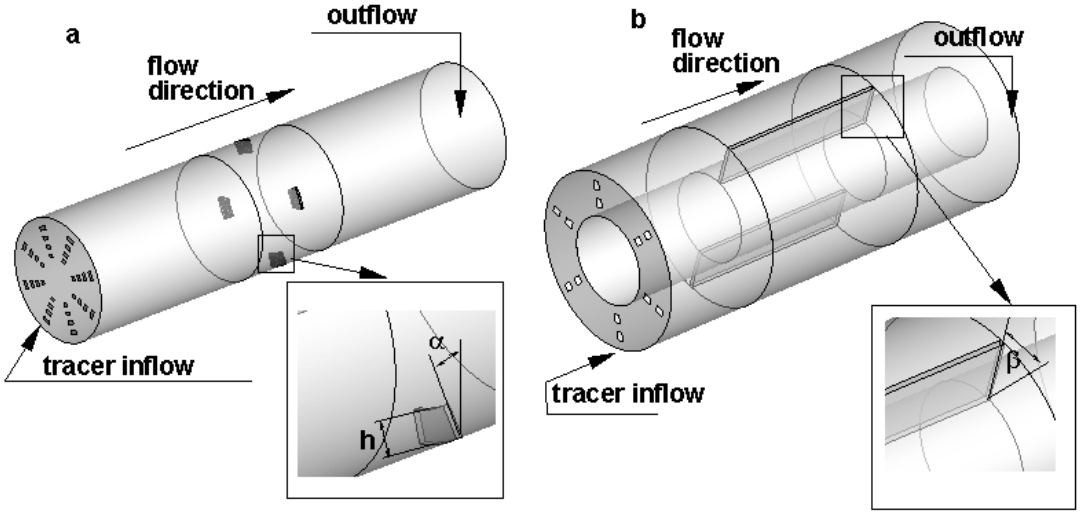

Figure 2: Initial static mixer configurations: a) HEV mixer, b) coaxial static mixer

The first configuration (Figure 2a) is allowed to change the fin height **h** and inclination **a** in the streamwise direction, while the second one is mapped into cylindrical coordinates and is free to change the shape of the blade, up a to a limit angle of **b**=60° respect to the streamwise flow..
Of the two mixer typologies chosen the first configuration is particularly tailored for Newtonian turbulent flows, while the second configuration is linked to a more general purpose static mixer and can be considered as a single elementary blade of multiple module configuration in heat transfer applications.
The design procedure was applied by accounting for a Newtonian fluid (water solution) and a Non-Newtonian pseudoplastic type corresponding to a peach puree with 15.7% w/w of solid contents (Steffe,1996), the rheological behavior of which being described by the power-law model, its consistency constant (k) and rheological behavior index (n) being equal to 4.5 Pa s^n and 0.35, respectively.
The flow regime resulted to be turbulent for the Newtonian liquid, but laminar for the power-law one, this changing dramatically the working behavior of the static mixer, as well as the effectiveness of the OSD procedure. In fact, the effect of Reynolds number is relevant depending on mixer configuration (Kumar 2007).

Table 1: Mixing index and Pressure drop in a HEV static mixer

Fluid	μ (Pa s)	K (Pa s^n)	n	Inlet Velocity (m/s)	Index M (best shape)	Pressure Drop (Pa)	Fin angle	Re at inflow
Newtonian	0.001			0.2	0.12	10	34.2°	9980
				0.4	0.10	26	25.2°	19960
				0.6	0.09	50	16.2°	29940
Non-Newtonian		4.5	0.35	0.2	0.73	302	25.5°	22
				0.4	0.85	442	35°	70
				0.6	0.78	580	45°	136

Table 1 results show that while in the Non-Newtonian case the application of OSD approach induces an improvement of the internal mixing (see the mixing index M, ranging from 1 to 0, the lower the better), in the Newtonian case the effects of application of the OSD are minimal.
Moreover, in the last case the reduction of fin height did not result in any improvement.
A different scenario was obtained in the case of the configuration shown in Figure 1b, where the application of OSD approach resulted in the final configuration showed in Figure 3a for the Newtonian case and in Figure 3b for the Non Newtonian one. The final objective function G for then Non-Newtonian case is 0.67 while in the Newtonian case is 0.86. Notice that the final shape is quite different between the two cases.

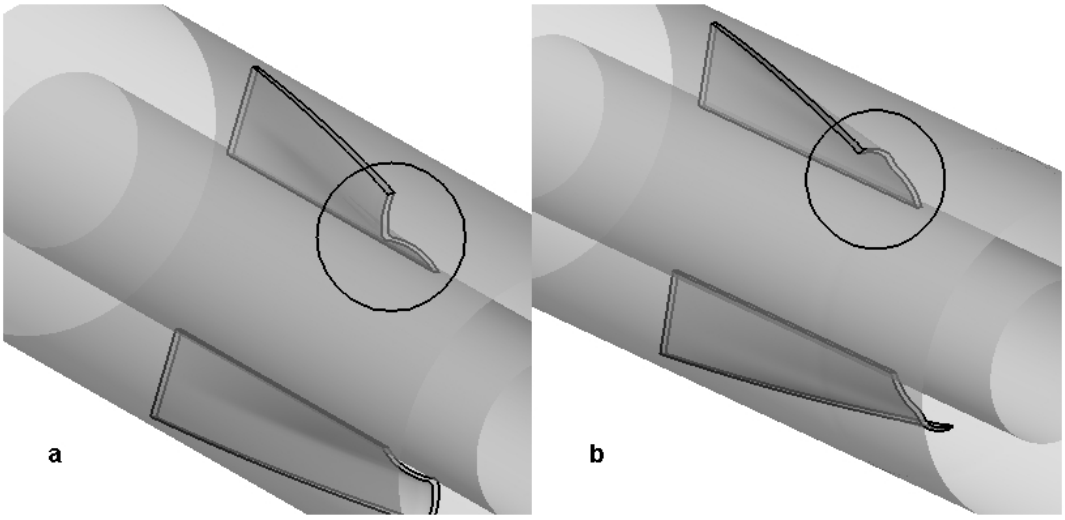

Figure 3: Optimal shapes for Newtonian (a) and Non-Newtonian (b) test cases.

Figure 4 shows the graph of the target function for the Non-Newtonian liquid once the optimal configuration had been obtained (point A), the objective function was modified by considering only the mixing efficiency term and neglecting the pressure drop term.

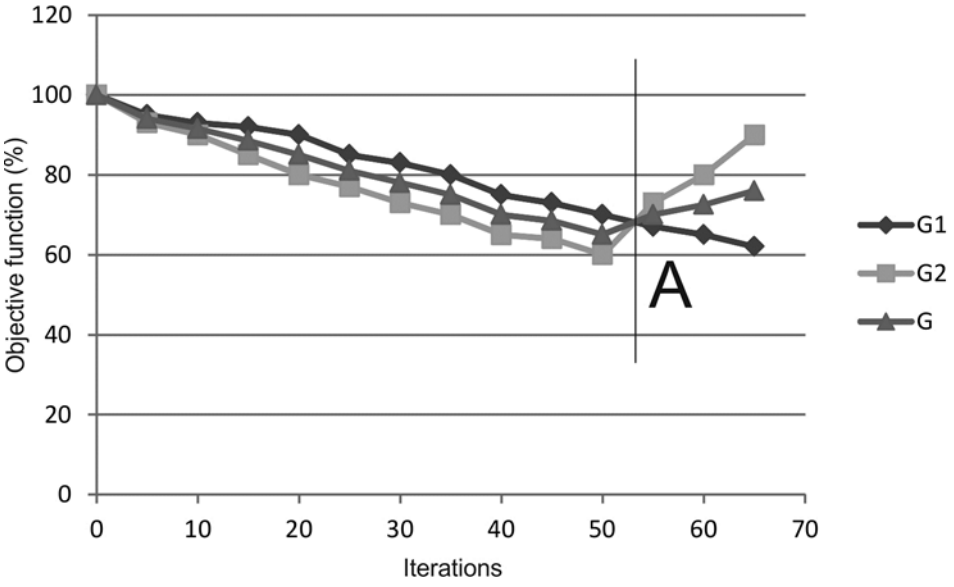

Figure 4: Normalized Objective function

By performing some other iteration, the mixing efficiency still tended to decrease, but in this case also the pressure drop increased, this confirming that point A was a real local minimum.

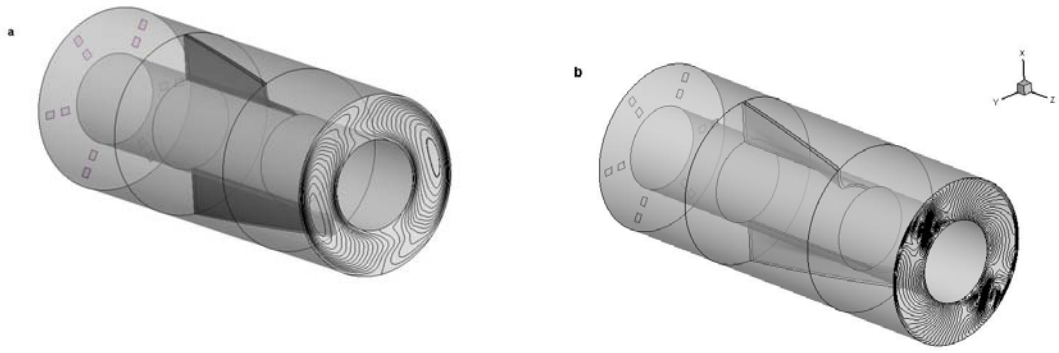

Figure 5: Contours of x-velocity at the outflow in two successive configurations (a= intermediate, b=final) for the Newtonian case

An other interesting remark is related to the major differences in the velocity profile for geometrical configurations quite similar between them, showed qualitatively on the outflow plane in Figure 5 for an intermediate and for the final geometry of the Newtonian case.

The main difference is due to the presence of two streamwise vortices in the final configuration which are missing in the configuration shown in Figure. 5a.

Following the work of Jeong & Hussain (1995), who stressed the need for Galilean-invariant vortex criteria, in a three-dimensional smooth velocity field v(x, t), an available Galilean-invariant vortex criteria use the velocity gradient decomposition:

$$\nabla v = S + \Omega \tag{22}$$

Where

$$S = \frac{1}{2}[(\nabla v) + (\nabla v)^T] \tag{23}$$

is the rate-of-strain tensor, and

$$S = \frac{1}{2}[(\nabla v) - (\nabla v)^T] \tag{24}$$

is the vorticity tensor.
Finally, according to the λ_2-criterion of Jeong & Hussain (1995), vortices can be detected as regions where

$$\lambda_2(S^2 + \Omega^2) < 0 \tag{25}$$

where $\lambda_2(A)$ denotes the intermediate eigenvalue of a symmetric tensor A. Under appropriate adiabatic assumptions, this last criterion guarantees an instantaneous local pressure minimum in a two- dimensional plane for Navier–Stokes flows. Using the λ_2-criterion, the 2 vortices shown in Figure 6 were detected.

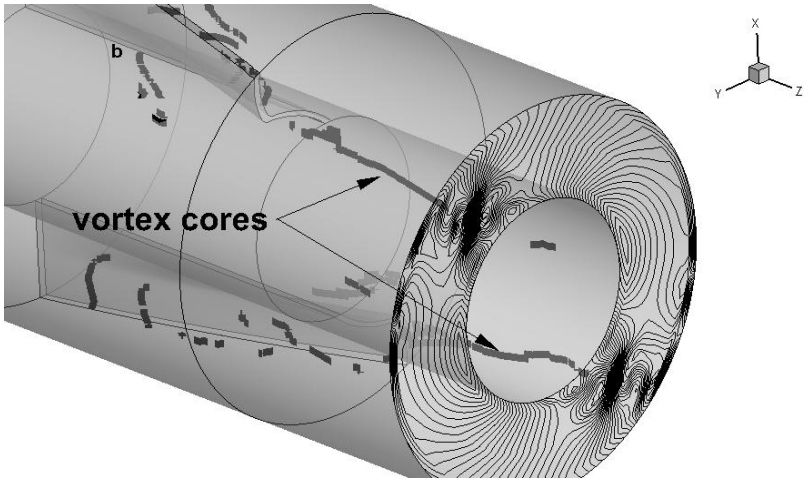

Figure 6: Vortex cores detected using the λ_2-criterion

4. Conclusions

While the OSD approach represents a powerful tool to optimize the shape of static mixers, the efficiency of the application strongly depends on the rheological of the fluid undergoing mixing and the conceptual design.
In case of geometrical configuration tailored for example for low-viscosity Newtonian flows as in HEV mixers (Ghanem et al., 2013) the improvement for the non-Newtonian case is negligible due to the inappropriate mixer theoretical configuration for this type of flows, Being an HEV mixer basically a trapezoidal vortex generator providing coherent structures similar to those found in natural turbulent boundary layers.
On the other hand, application of OSD approach in coaxial mixers for the case of non-Newtonian flow induced an enhanced mixing still maintaining a certain control over the pressure drop, Such technology can be tailored for

each class of fluid and applied on a case by case approach by using manufacturing technologies like for example rapid prototyping.
Several issues remain open, for example the choice of the tracer inflow distribution, chosen in an arbitrary way, can affect the area interested by the tracer diffusion and as a consequence the calculation of the mixing index at the outflow, as well as the existence of a unique solution of the optimization problem.
Moreover, the volumetric flow rate plays of course an important role, as optimal geometries are strongly relates to the fluid dynamic regime, meaning that the optimization should be performed considering the process parameter and not only the rheological properties of the fluid involved.
Results showed that Optimal Shape Design technique represents a powerful technique which can be used to increase the efficiency of any process in which the shape of a mechanical parts plays a fundamental role.

References

Burton I. E., 1998, Comparison of SIMPLE- and PISO-type algorithms for transient flows, International Journal of Numerical Methods in Fluids, 26, 4, 459-483.

Byrde, O., Sawley, M.L., 1999. Optimization ofa Kenics static mixer for non-creeping flow conditions. Chemical Engineering Journal 72, 163–169.

Farin G., Curves and Surfaces for Computer Aided Geometric Design. 2001. 5th ed. Boston: Academic Press.,USA.

Fourcade, E., Wadley, R., Hoefsloot, H.C., Green, A., Iedema, P.D., 2001. CFD calculation oflaminar striation thinning in static mixer reactors. Chemical Engineering Science 56, 6729–6741.

Ghanem A., Habchi C. , Lemenand T., Della Valle D., Peerhossaini H., 2013, Energy efficiency in process industry – High-efficiency vortex (HEV) multifunctional heat exchanger, Renewable Energy, 56, 96–104.

Hobbs, D.M., Muzzio, F.J., 1998a. Optimization ofa static mixer using dynamical systems techniques. Chemical Engineering Science 53, 3199–3213.

Hobbs, D.M., Muzzio, F.J., 1998b. Reynolds number effects on laminar mixing in the Kenics static mixer. Chemical Engineering Journal 70, 93–104.

Hobbs, D.M., Swanson, P.D., Muzzio, F.J., 1998. Numerical characterization oflow Reynolds number flow in the Kenics static mixer. Chemical Engineering Science 53, 1565–1584.

Keller C. T.,1998, Iterative Methods for Optimization, in Frontiers in Applied Mathematics, SIAM.

Kumar V., Shirke V., Nigam K.D.P., 2008, Performance of Kenics static mixer over a wide range of Reynolds number, Chemical Engineering Journal, 139, 2, ,284-295.

Issa R. I., 1986, Solution of the Implicitly Discretised Fluid Flow Equations by Operator Splitting, J. Comput. Phys., 62, 40–65.

Jeong, J. & Hussain, F., 1995, On the identification of a vortex. J. Fluid. Mech. 285, 69–94.

Mohammadi B., Pironneau O., 2001, Applied Shape Optimization for Fluids. Oxford, Oxford Univ. Press.

Mohammadi B., Pironneau O., 2004, Shape optimization in fluid mechanics, Annual Review Fluid Mech., 36:11.1–11.25.

Mutsakis M., Streiff F.A., Schneider G., 1986, Advances in Static Mixing Technology, Chem. Eng. Prog., 82, 7, 42-48.

Nocedal, J., Wright S. , 2006, Numerical Optimization. Series: Springer Series in Operations Research and Financial Engineering, 2nd ed.

OpenFoam, The free CFD Toolbox, www.openfoam.org. , accessed 20.04.2013

Patankar, S. V. and Spalding, D.B., 1972, A calculation procedure for heat, mass and momentum transfer in three-dimensional parabolic flows, Int. J. of Heat and Mass Transfer, 15, 10, 1787-1806.

Rauline D., Le Blévec J.-M., Bousquet J., Tanguy P.A., 2000, A Comparative Assessment of the Performance of the Kenics and SMX Static Mixers, Chemical Engineering Research and Design, 78, A3 Special issue in Fluid Mixing, 389-396.

Rauline D., Tanguy P.A., Le Blevec J.M., Bousquet J.,1998, Numerical investigation of the performance of several static mixers, Canadian Journal of Chemical Engineering, 76, 3, 527-535.

Sarghini, F., U. Piomelli,, Balaras E., 1999, Scale-Similar Models for Large-Eddy Simulations, Physics of Fluids, 11, 6, 1596.

Sarghini, F., De Felice, G., Santini, S., 2003, Neural networks based subgrid scale modeling in large-eddy simulations, Computers and Fluids, 32,1, 97-108

Sokolowski J., Zolezio J.P., 1991. Introduction to shape optimization. Shape sensitivity analysis. Springer Series Comput. Math. 16.5-12.

Steffe J.F., 1996. Rheological Methods in Food Process Engineering, 2nd edition, Freeman Press, East Lansing, MI, USA.
Szalai, E.S., Muzzio, F.J., 2003. Fundamental approach to the design andoptimization ofstatic mixers. A.I.Ch.E. Journal 49, 2687–2699.
Tartar L., 1974. Control problems in the coefficients of PDE, Lecture notes in Economics and Math Systems. A. Bensoussan, Springer Verlag.
Thakur, R. K., Vial, C., Nigam, K. D. P., Nauman, E. B., & Djelveh, G., 2003, Static mixers in the process industries—a review. Chemical Engineering Research and Design, 81(7), 787-826.
van Wageningen, W.F.C., Kandhai, D., Mudde, R.F., van den Akker, H.E.A., 2004. Dynamic flow in a Kenics static mixer: an assessment of various CFD methods. A.I.Ch.E. Journal 50, 1684–1696.